Electronic Supplementary Material (ESI) for Catalysis Science & Technology.

Supplementary Information for:

Nanostructured Ni-Cu Electrocatalysts for the Oxygen Evolution Reaction

Rajendra P. Gautam, Hanqing Pan, Farzaneh Chalyavi,

Matthew J. Tucker, and Christopher J. Barile*

Department of Chemistry, University of Nevada, Reno, NV 89557

*E-mail: cbarile@unr.edu

Supplementary Figures

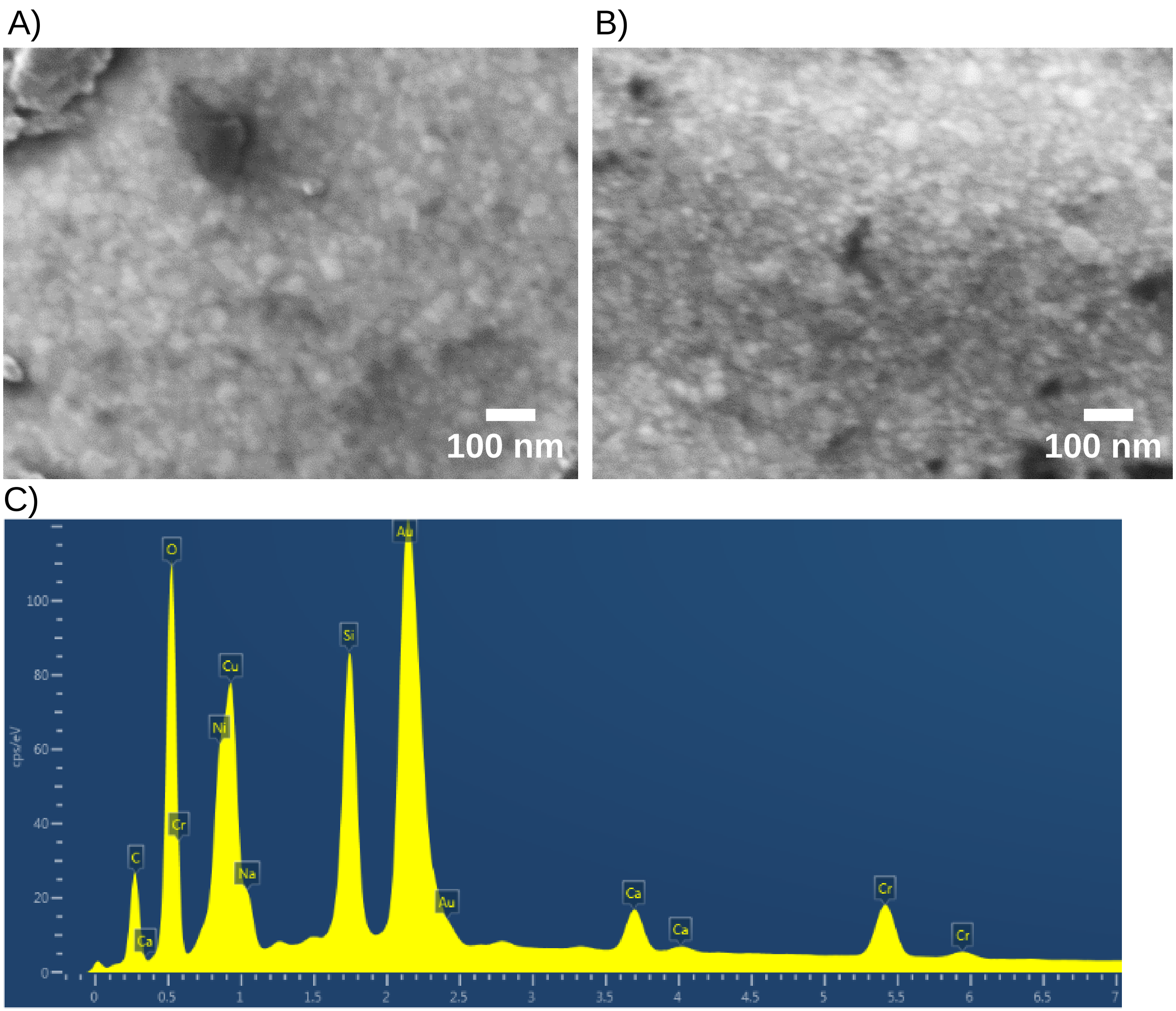

Figure S1: SEM images of 46:54 mol % (A) and 71:29 mol % (B) Ni-Cu NPs. Representative energy-dispersive X-ray (EDX) spectrum of Ni-Cu bimetallic nanoparticles on a 100 nm-thick Au on Cr on glass substrate (C). The elements detected are Ni, Cu, Au, Cr, O, C, Si, Ca, and Na. The Au, Cr, O, Si, Ca, and Na detected is from the substrate. C is a common impurity detected in EDS measurements.

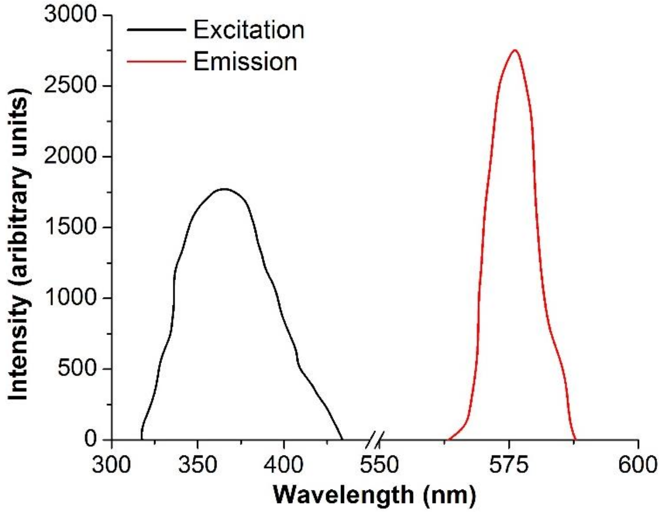

Figure S2: Fluorescence spectra of Cu nanoclusters.

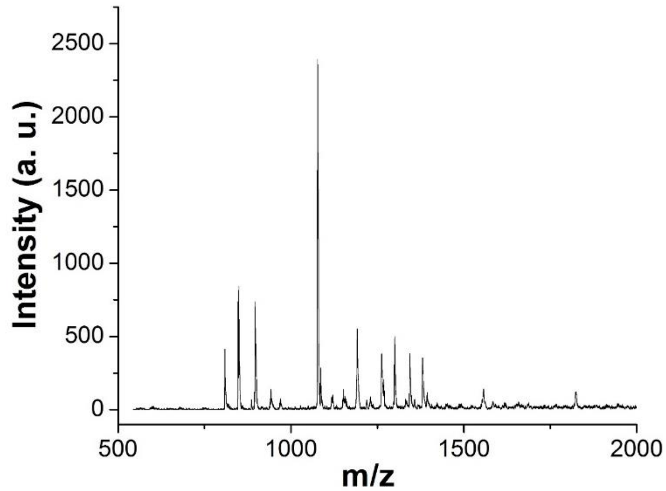

Figure S3: The positive-mode MALDI-TOF MS of the as synthesized 100 mol % Cu nanoclusters.

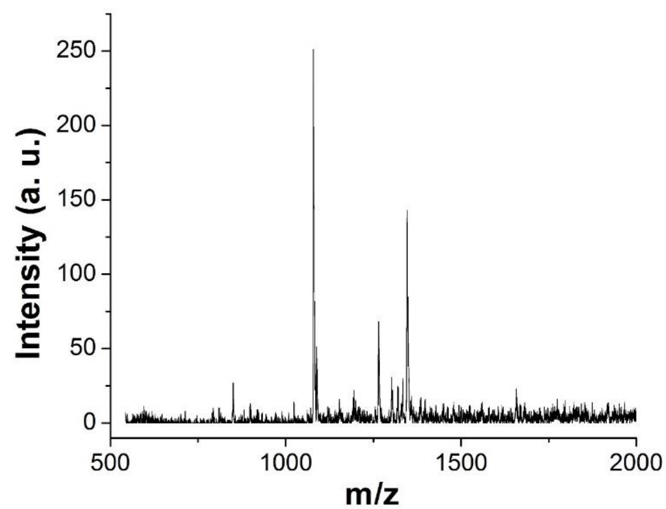

Figure S4: The positive-mode MALDI-TOF MS of the as synthesized 25:75 mol % Ni-Cu nanoclusters.

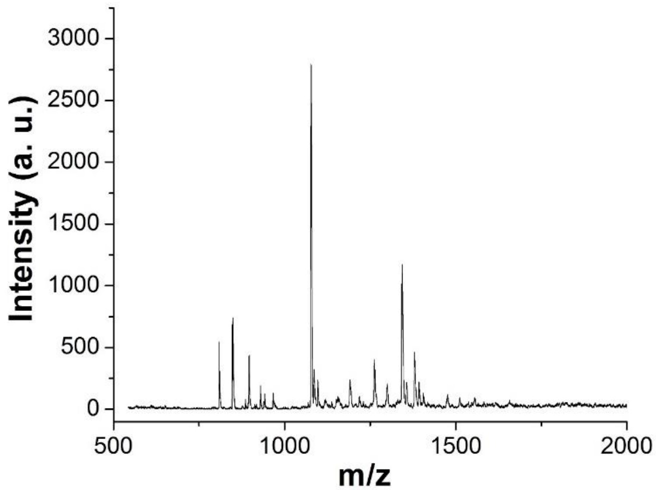

Figure S5: The positive-mode MALDI-TOF MS of the as synthesized 43:57 mol % Ni-Cu nanoclusters.

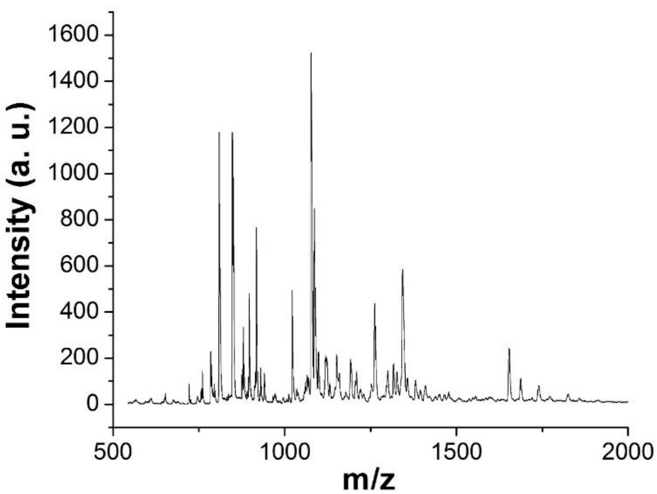

Figure S6: The positive-mode MALDI-TOF MS of the as synthesized 100 mol % Ni nanoclusters.

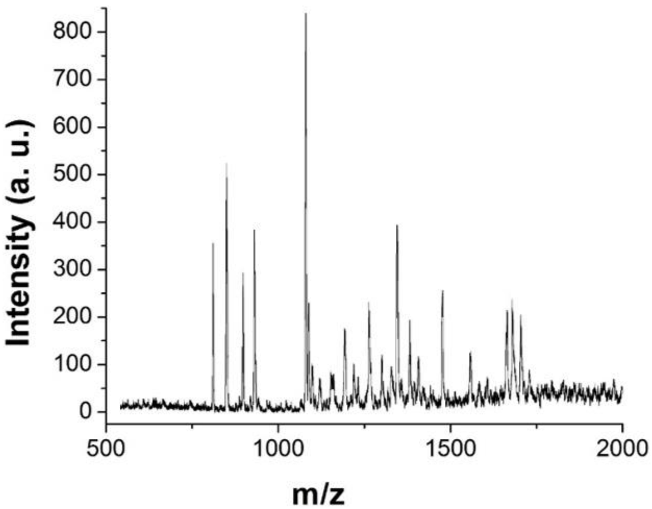

Figure S7: Positive-mode MALDI-TOF mass spectrum of the 52:48 mol % Ni-Cu nanoclusters after being immersed overnight in 1 M NaOH and washed with water.

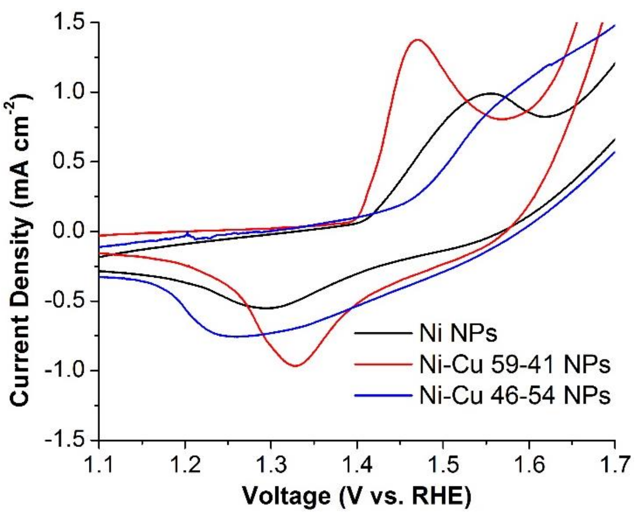

Figure S8: Cyclic voltammetry at a scan rate of 10 mV s^{-1} of glassy carbon electrodes modified with Ni nanoparticles (black line), 59:41 mol % Ni-Cu nanoparticles (red line), and 46:54 mol % Ni-Cu nanoparticles (blue line) along with Vulcan XC-72 and PVDF.

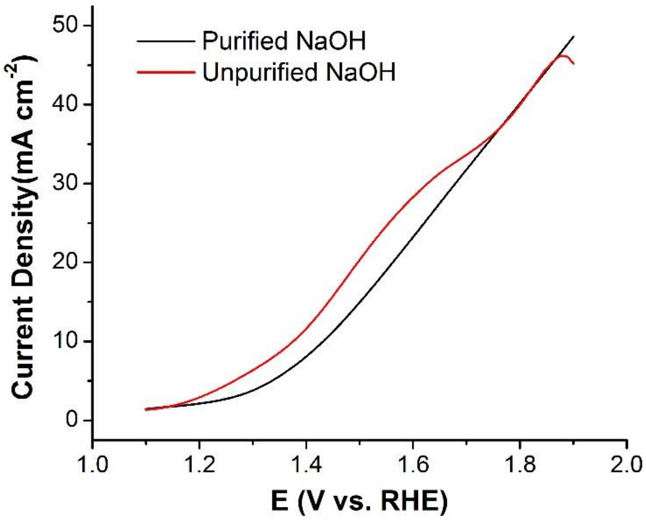

Figure S9: Linear sweep voltammograms of the oxygen evolution reaction in purified (2 ppb Fe, black line) and unpurified (115 ppb Fe, red line) 1 M NaOH using a glassy carbon electrode modified with a mixture of 52:48 mol % Ni-Cu nanoclusters, Vulcan XC-72, and PVDF at a scan rate of 10 mV s^{-1}.

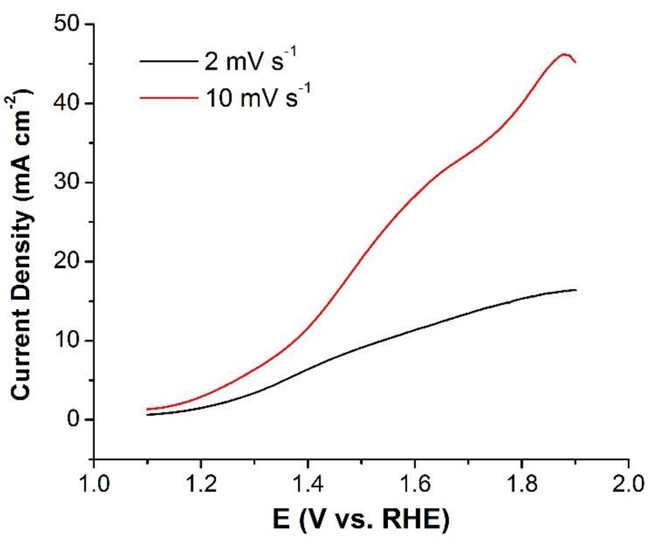

Figure S10: Linear sweep voltammograms of the oxygen evolution reaction in 1 M NaOH at a scan rate of 2 mV s^{-1} (black line) and 10 mV s^{-1} (red line) on glassy carbon electrodes modified with 52:48 mol % Ni-Cu nanoclusters, Vulcan XC-72, and PVDF.

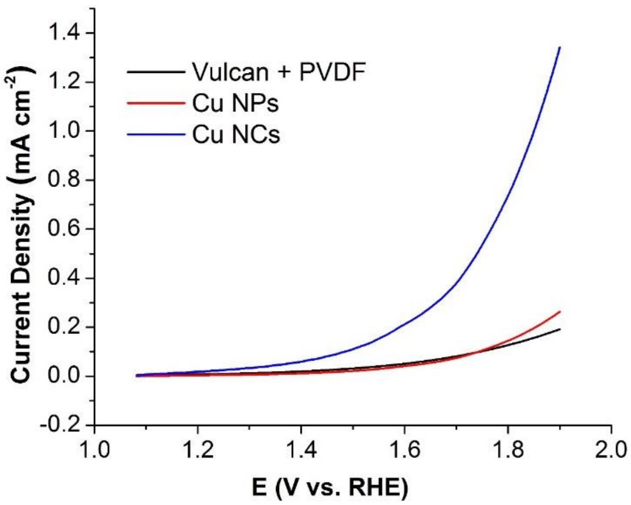

Figure S11: Linear sweep voltammograms of the oxygen evolution reaction in 1 M NaOH on glassy carbon working electrodes that have been modified with Cu nanoclusters (100 mol % Cu NCs, blue line) and Cu nanoparticles (100 mol % Cu NPs, red line). A control with the electrode modified with only Vulcan XC-72 and PVDF is also shown (black line).

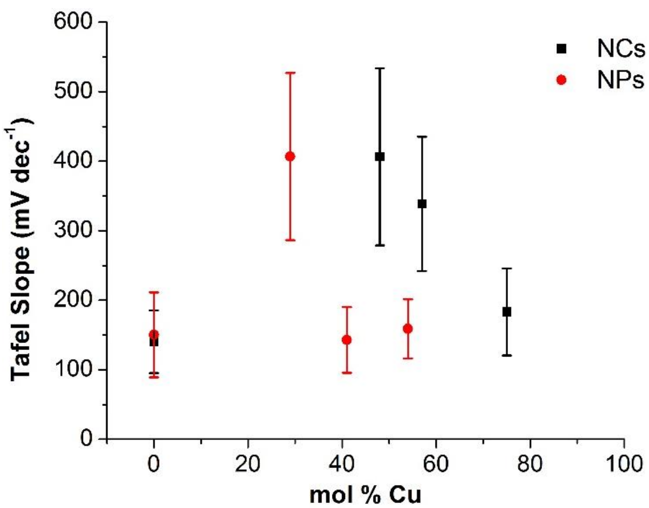

Figure S12: Tafel slopes calculated from linear sweep voltammograms of the oxygen evolution reaction in 1 M NaOH on glassy carbon working electrodes that have been modified with nanoclusters (NCs, black line) and nanoparticles (NPs, red line).

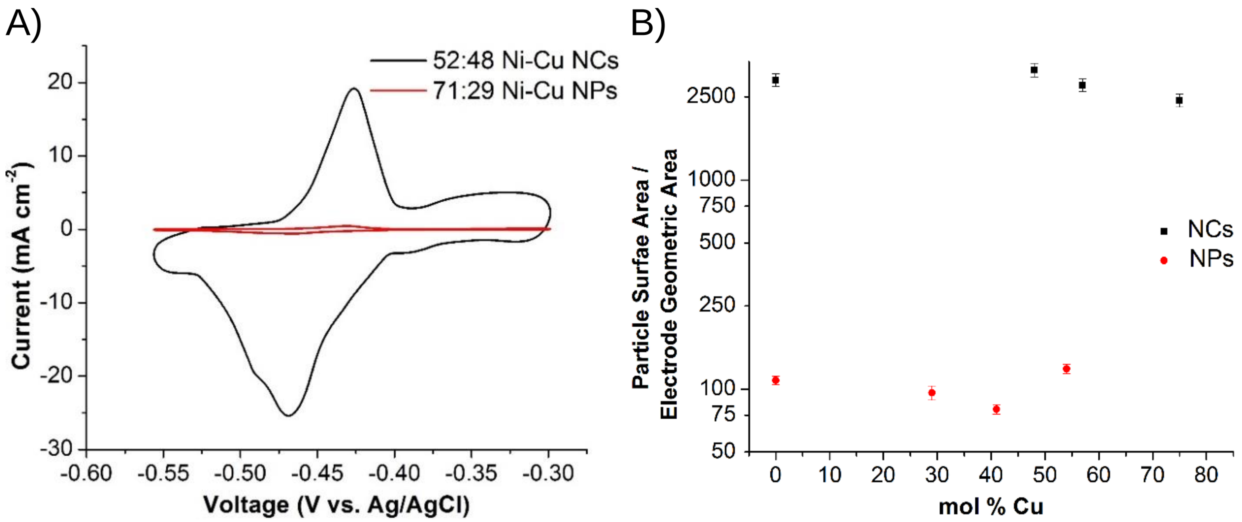

Figure S13: Pb UPD experiments of nanoclusters (black) and nanoparticles (red) in an Ar-sparged solution containing 100 mM $HClO_4$, 1 mM $Pb(ClO_4)_2$, and 20 mM KCl at a scan rate of 10 mV/s (A). Calculated electrochemically active surface areas of the nanoclusters (black) and nanoparticles (red) as a function of Cu composition in the catalysts (B).

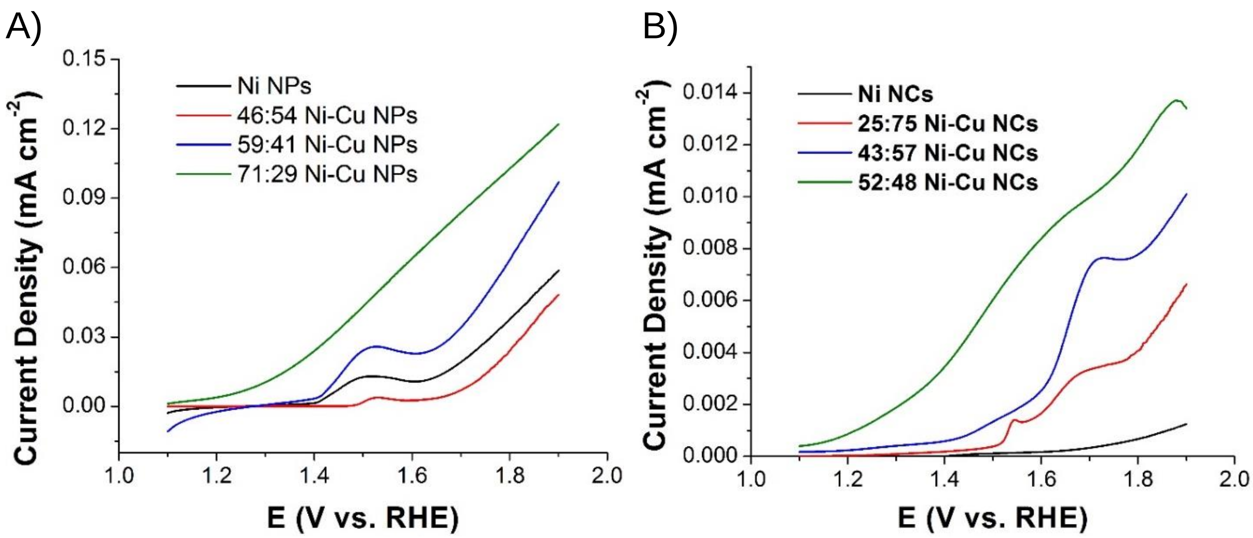

Figure S14: Linear sweep voltammograms at 10 mV s^{-1} of the oxygen evolution reaction in 1 M NaOH using a glassy carbon working electrode modified with a mixture of Ni-Cu bimetallic nanoparticles (NPs, A) or nanoclusters (NCs, B), Vulcan XC-72, and PVDF. Ni-Cu bimetallic NPs and NCs with various molar ratios were tested (colored lines) along with pure Ni NPs and NCs (black lines). Current densities are reported against the electrochemically active surface areas reported in Figure S9.

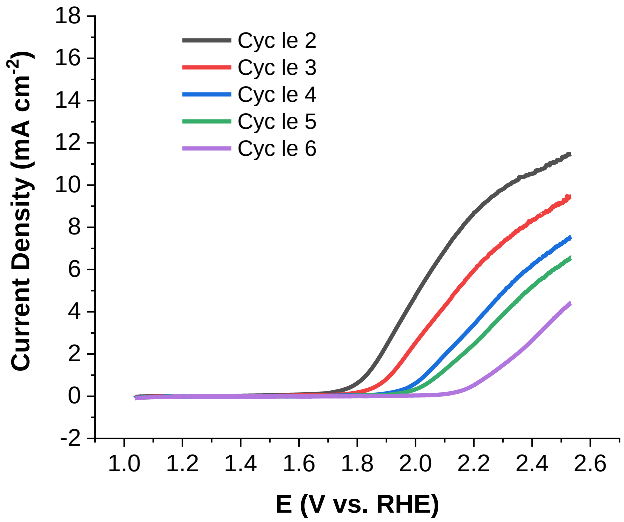

Figure S15: Linear sweep voltammograms of multiple cycles of the oxygen evolution reaction in 1 M NaOH using 52:48 mol % Ni-Cu nanoclusters.

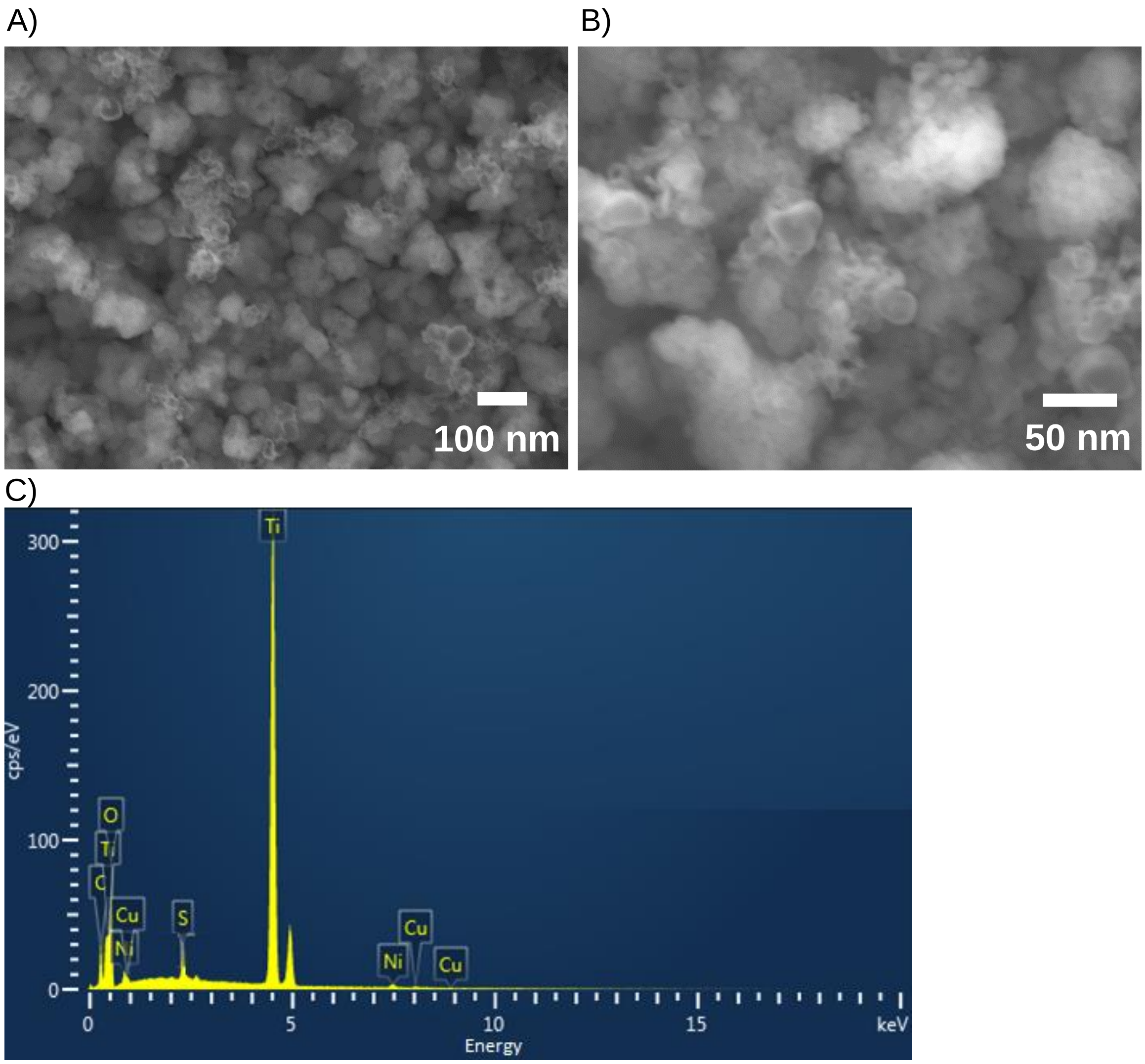

Figure S16: SEM images of an electrode containing 52:48 mol % Ni-Cu nanoclusters on TiO_2 nanoparticles on carbon paper (A, B). The EDX spectrum of the electrode (C) demonstrates the presence of Ni and Cu from the core of the Ni-Cu nanoclusters, S from the glutathione ligand of the nanoclusters, and Ti and O from the TiO_2 nanoparticles.

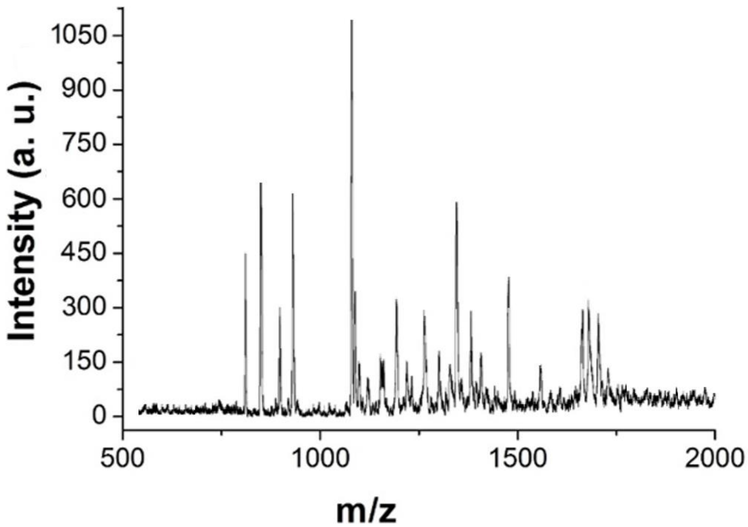

Figure S17: Positive-mode MALDI-TOF mass spectrum of the 52:48 mol % Ni-Cu nanoclusters after OER catalysis at 10 mA cm^{-2} for 1 hr.

Assignment	m/z Calculated	100% Cu	25%:75% Ni:Cu	43:57 Ni:Cu	52:48 Ni:Cu	100% Ni
$[Cu_2Ni_2GS + Na]^+$ or $[Cu_9 + H]^+$ or $[Cu_5Ni_4 + Na]^+$ or $[Cu_3NiGS + Na]^+$	572.79 or 573.37 or 575.37 or 577.79				575.5 (18%)	
$[CuNi_{10} + Na]^+$ or **$[Cu_3Ni_3GS + H]^+$** or **$[Cu_6Ni_5 + H]^+$** or **$[Cu_2Ni_9 + Na]^+$**	673.26 or 673.67 or 674.25 or 676.26				673.8 (15%)	
$[Cu_3GS_2 + H]^+$	803.95	806.5 (18%)				
$[Cu_2Ni_6GS + Na]^+$ or **$[Cu_9Ni_4 + H]^+$** or **$[Cu_5Ni_8 + Na]^+$** or **$[Cu_7NiGS + H]^+$**	806.53 or 807.11 or 809.11 or 809.52			807.9 (20%)		
$[Ni_3GS_2 + Na]^+$	810.94					809.7 (78%)
$[Cu_5Ni_8 + Na]^+$ or $[Cu_7NiGS + H]^+$ or $[Ni_3GS_2 + Na]^+$ or $[Cu_3Ni_5GS + Na]^+$ or $[Cu_{10}Ni_3 + H]^+$	809.11 or 809.52 or 810.94 or 811.52 or 812.1				811.0 (32%)	
$[Ni_4GS_2 + H]^+$	846.9					846.5 (77%)
$[Cu_5Ni_9 + H]^+$ or $[Ni_4GS_2 + H]^+$ or $[Cu_3Ni_6GS + H]^+$ or $[Cu_6Ni_8 + H]^+$	845.06 or 846.9 or 849.47 or 850.05			847.6 (26%)	847.6 (59%)	
$[Ni_4GS_2 + H]^+$ or $[Cu_3Ni_6GS + H]^+$ or $[Cu_6Ni_8 + H]^+$ or $[CuNi_3GS_2 + H]^+$	846.9 or 849.47 or 850.05 or 851.89		849.3 (11%)			
$[Ni_{10}GS + H]^+$	892.42					895.4 (32%)
$[Cu_8NiGS + Na]^+$ or **$[CuNi_9GS + H]^+$**	896.43 or 897.42			896.6 (16%)	897.9 (32%)	
$[Cu_9GS + Na]^+$	901.43	899.5 (31%)				
$[Ni_{10}GS + Na]^+$	914.41					916.3 (50%)
$[Ni_5GS_2 + Na]^+$	926.81					927.9 (11%)
$[Cu_5Ni_{10} + Na]^+$ or $[Cu_7Ni_3GS + H]^+$ or $[Cu_{10}Ni_5 + H]^+$ or $[Cu_3Ni_7GS + Na]^+$ or $[Cu_5GS_2 + H]^+$ or $[Cu_6Ni_9 + Na]^+$ or $[Cu_8Ni_2GS + H]^+$ or $[CuNi_4GS_2 + Na]^+$	926.97 or 927.39 or 929.97 or 929.39 or 929.81 or 931.97 or 932.38 or 931.81				929.9 (59%)	
$[Ni_7GS_2 + H]^+$	1022.7					1020.9 (32%)
$[Cu_8Ni_4GS + Na]^+$ or **$[Cu_6NiGS_2 + Na]^+$**	1072.23 or 1074.65			1073.9 (100%)		
$[Cu_7GS_2 + Na]^+$	1079.65	1077.0 (100%)				
$[Cu_9Ni_3GS + Na]^+$ or $[Cu_7GS_2 + Na]^+$	1077.23 or 1079.65				1078.5 (100%)	
$[Cu_9Ni_3GS + Na]^+$ or $[Cu_7GS_2 + Na]^+$ or $[Cu_{10}Ni_2GS + Na]^+$ or $[Ni_8GS_2 + H]^+$	1077.23 or 1079.65 or 1082.22 or 1082.63		1079.9 (100%)			

$[Ni_8GS_2 + H]^+$	1082.63					1082.5 (100%)
$[Ni_8GS_2 + H]^+$ or $[Cu_3Ni_{10}GS + H]^+$ or $[CuNi_7GS_2 + H]^+$ or $[Cu_4Ni_9GS + H]^+$	1082.63 or 1083.21 or 1087.63 or 1088.21			1085.5 (12%)		
$[CuNi_7GS_2 + H]^+$ or **$[Cu_4Ni_9GS + H]^+$**	1087.63 or 1088.21		1089.0 (20%)			
$[CuNi_7GS_2 + H]^+$ or **$[Cu_4Ni_9GS + H]^+$** or **$[Cu_2Ni_6GS_2 + H]^+$**	1087.63 or 1088.21 or 1092.62				1089.9 (30%)	
$[Ni_3GS_3 + H]^+$	1095.04					1095.1 (56%)
$[Cu_3Ni_5GS_2 + H]^+$ or **$[CuNi_2GS_3 + H]^+$** or **$[Cu_6Ni_7GS + H]^+$** or **$[Cu_9Ni_9 + H]^+$** or **$[Cu_4Ni_4GS_2 + H]^+$**	1097.62 or 1100.03 or 1098.2 or 1100.77 or 1100.61				1099.1 (13%)	
$[Ni_3GS_3 + Na]^+$	1117.02					1118.6 (14%)
$[Cu_3NiGS_3 + Na]^+$ or $[Cu_6Ni_3GS_2 + Na]^+$ or $[Cu_9Ni_5GS + Na]^+$ or $[Cu_4GS_3 + Na]^+$	1189.94 or 1192.52 or 1193.1 or 1194.93				1192.8 (23%)	
$[CuNi_4GS_3 + H]^+$ or $[Cu_4Ni_6GS_2 + H]^+$ or $[Cu_7Ni_8GS + H]^+$ or $[Ni_{10}GS_2 + Na]^+$ or $[Cu_2Ni_3GS_3 + H]^+$ or $[Cu_{10}Ni_{10} + H]^+$	1217.9 or 1218.48 or 1221.06 or 1220.48 or 1222.9 or 1221.64				1220.3 (13%)	
$[CuNi_{10}GS_2 + H]^+$ or **$[Cu_9NiGS_2 + Na]^+$**	1263.43 or 1265.44		1264.8 (27%)	1262.8 (14%)	1263.7 (30%)	
$[Cu_6GS_3 + H]^+$	1300.81	1299.8 (21%)				
$[CuNi_5GS_3 + Na]^+$ or $[Cu_4Ni_7GS_2 + Na]^+$ or $[Cu_7Ni_9GS + Na]^+$ or $[Cu_6GS_3 + H]^+$ or $[Cu_2Ni_4GS_3 + Na]^+$ or $[Cu_9Ni_2GS_2 + H]^+$	1297.82 or 1300.39 or 1300.97 or 1300.81 or 1302.81 or 1301.39				1300.3 (16%)	
$[Cu_7Ni_9GS + Na]^+$ or $[Cu_6GS_3 + H]^+$ or $[Cu_2Ni_4GS_3 + Na]^+$ or $[Cu_9Ni_2GS_2 + H]^+$ or $[Cu_5Ni_6GS_2 + Na]^+$ or $[Cu_8Ni_8GS + Na]^+$ or $[Cu_{10}NiGS_2 + H]^+$	1300.97 or 1300.81 or 1302.81 or 1301.39 or 1305.39 or 1305.97 or 1306.39		1303.7 (12%)			
$[Cu_5NiGS_3 + Na]^+$ or **$[Cu_8Ni_3GS_2 + Na]^+$**	1317.8 or 1318.38		1319.6 (10%)			
$[Cu_2Ni_{10}GS_2 + H]^+$ or $[Cu_{10}NiGS_2 + Na]^+$ or $[Ni_7GS_3 + H]^+$	1326.36 or 1328.37 or 1328.78				1327.7 (13%)	
$[Cu_3Ni_9GS_2 + H]^+$ or **$[CuNi_6GS_3 + H]^+$**	1331.35 or 1333.77		1333.3 (12%)			
$[Cu_5Ni_7GS_2 + H]^+$ or **$[Cu_8Ni_9GS + H]^+$** or **$[Cu_3Ni_4GS_3 + H]^+$** or **$[Cu_6Ni_6GS_2 + H]^+$**	1341.34 or 1341.92 or 1343.76 or 1346.34				1343.8 (57%)	
$[Cu_9Ni_8GS + H]^+$ or **$[Cu_8Ni_9GS + H]^+$** or **$[Cu_3Ni_4GS_3 + H]^+$** or **$[Cu_6Ni_6GS_2 + H]^+$**	1346.92 or 1341.92 or 1343.76 or 1346.34			1344.5 (42%)		
$[Cu_2Ni_{10}GS_2 + Na]^+$ or **$[Cu_9Ni_8GS + H]^+$** or **$[Cu_4Ni_3GS_3 + H]^+$** or **$[Cu_6Ni_6GS_2 + H]^+$**	1348.34 or 1346.92 or 1348.75 or 1346.34		1347.0 (57%)			

[$Cu_8Ni_4GS_2$ + Na]$^+$ or **[Cu_6NiGS_3 + Na]$^+$**	1378.31 or 1380.73			1379.5 (16%)		
[Cu_6NiGS_3 + Na]$^+$ or **[$Cu_9Ni_3GS_2$ + Na]$^+$**	1380.73 or 1383.3				1382.6 (25%)	
[$Cu_3Ni_5GS_3$ + H]$^+$ or **[$Cu_6Ni_7GS_2$ + H]$^+$** or **[Cu_9Ni_9GS + H]$^+$**	1403.69 or 1404.27 or 1406.85				1405.5 (16%)	
[$Cu_4Ni_{10}GS_2$ + Na]$^+$ or [$Cu_6Ni_3GS_3$ + H]$^+$ or [$Cu_2Ni_7GS_3$ + Na]$^+$ or [$Cu_9Ni_5GS_2$ + H]$^+$ or [$Cu_5Ni_9GS_2$ + Na]$^+$ or [Cu_4GS_4 + H]$^+$ or [$Cu_7Ni_2GS_3$ + H]$^+$ or [Ni_4GS_4 + Na]$^+$	1476.2 or 1476.61 or 1478.61 or 1477.19 or 1481.19 or 1479.03 or 1481.61 or 1481.03				1478.7 (23%)	
[$Cu_3Ni_2GS_4$ + Na]$^+$ or **[$Cu_6Ni_4GS_3$ + Na]$^+$** or **[$Cu_9Ni_6GS_2$ + Na]$^+$** or **[Cu_4NiGS_4 + Na]$^+$** or **[$Cu_7Ni_3GS_3$ + Na]$^+$**	1555.95 or 1556.53 or 1559.11 or 1560.94 or 1561.52				1558.7 (20%)	
[$CuNi_6GS_4$ + Na]$^+$ or **[$Cu_8Ni_4GS_3$ + H]$^+$** or **[$Cu_4Ni_8GS_3$ + Na]$^+$** or **[Cu_6NiGS_4 + H]$^+$** or **[$Cu_2Ni_5GS_4$ + Na]$^+$**	1661.83 or 1662.4 or 1664.41 or 1664.82 or 1666.82				1663.9 (22%)	
[$Cu_9Ni_8GS_2$ + Na]$^+$ or **[$Cu_7Ni_5GS_3$ + Na]$^+$** or **[$Cu_5Ni_2GS_4$ + Na]$^+$** or **[$Cu_{10}Ni_7GS_2$ + Na]$^+$**	1676.97 or 1679.39 or 1681.81 or 1679.97				1679.9 (24%)	
[$Cu_2Ni_6GS_4$ + H]$^+$ or **[$Cu_5Ni_8GS_3$ + H]$^+$** or **[$Cu_8Ni_{10}GS_2$ + H]$^+$**	1704.77 or 1705.35 or 1707.93				1705.0 (22%)	
[$Cu_{10}Ni_3GS_3$ + H]$^+$ or **[$Cu_2Ni_6GS_4$ + Na]$^+$** or **[$Cu_9Ni_4GS_3$ + H]$^+$** or **[$Cu_5Ni_8GS_3$ + Na]$^+$** or **[Cu_7NiGS_4 + H]$^+$** or **[$Cu_8Ni_{10}GS_2$ + Na]$^+$**	1726.76 or 1725.33 or 1727.34 or 1729.75 or 1729.91 or 1730.33				1727.9 (12%)	
[$Cu_6Ni_8GS_3$ + Na]$^+$ or **[Cu_8NiGS_4 + H]$^+$** or **[$Cu_4Ni_5GS_4$ + Na]$^+$** or **[$Cu_9Ni_{10}GS_2$ + Na]$^+$**	1792.26 or 1792.68 or 1794.68 or 1792.84				1794.2 (25%)	
[$Cu_7Ni_{10}GS_3$ + Na]$^+$ or **[$Cu_9Ni_3GS_4$ + H]$^+$** or **[$Cu_5Ni_7GS_4$ + Na]$^+$**	1973.06 or 1973.48 or 1975.48				1974.8 (10%)	

Table S1: MALDI-TOF peak assignments for Cu, Ni, and Ni-Cu nanoclusters. Assignments in **bold** are peaks that can only be ascribed to a bimetallic species. Assignments in blue are bimetallic species detected in the spectra of all three bimetallic nanoclusters compositions. Normalized peak intensities are listed in parenthesis after each found m/z value. Peaks were considered present if they possessed a normalized intensity of at least 10%. Peaks were assigned to a species if the calculated m/z value for the isotopically most abundant peak matched within 3 amu.

Catalyst	Electrolyte	Onset E (V_{RHE})	Onset overpotential (V_{RHE} – 1.23 V)	Overpotential (mV) at specific current density	Reference
Precious metal					
Ru_{60}-Co_{40}	0.1 M $HClO_4$	1.41	0.18	-	4
Ru_{70}-Ir_{30}	0.1 M $HClO_4$	1.40	0.27	-	4
RuO_2	0.1 M KOH	1.44	0.21	425 @ 20 mA/cm^2	5
IrO_2	1 M KOH	1.51	0.28	340 @ 10 mA/cm^2	6
Spinel family					
$CoFe_2O_4$ on GCE	0.1 M KOH	1.58	0.35	443 @ 10 mA/cm^2	7
Mn_3O_4 on GCE	1 M KOH	1.68	0.45	>600 @ 3 mA/cm^2	8
Co_3O_4 on Au	1 M KOH	1.56	0.33	400 @ 10 mA/cm^2	9
$Mn_{2.1}Co_{0.9}O_4$	1 M KOH	1.64	0.41	490 @ 3 mA/cm^2	8
$ZnCo_2O_4$ on Pt	1 M KOH (pH 13.8)	1.62	0.39	450 @ 20 mA/cm^2	10
$NiCo_2S_4$ nanostructure	1 M KOH	1.50	0.27	260 @ 10 mA/cm^2	24
FeCo oxide on Ni foam	1 M KOH	1.49	0.26	205 @ 10 mA/cm^2	25
Layer-structure type family					
CoOOH on PtO/AuO	0.1 M KOH/LiOH	1.48	0.25	450 @ 5 mA/cm^2	11
3D Ni-Fe LDH on Ni foam	0.1 M KOH	1.46	0.23	280 @ 30 mA/cm^2	12
Co-Ni LDH on FTO	0.1 M potassium phosphate (pH 7)	1.623	0.393	490 @ 1 mA/cm^2	13
Co-Co LDH	0.1 M potassium phosphate (pH 7)	1.638	0.408	610 @ 1 mA/cm^2	13
Zn-Co LDH on GCE	0.1 M KOH (pH 13)	1.57	0.34	-	14
Co-Fe LDH (1:0.35) on GCE	0.1 M KOH	1.52	0.29	350 @ 10 mA/cm^2	15
Co-Cr LDH (2:1) on GCE	0.1 M KOH	1.47	0.24	340 @ 10 mA/cm^2	5
Ni-Fe-Mn LDH on CFP	1 M KOH	1.43	0.20	289 @ 20 mA/cm^2	16

β–$Ni(OH)_2$ nanoparticle film	0.1 M KOH	1.55	0.32	450 @ 30 mA/cm^2	12
Co-Ni based nanotubes/nanosheets on Cu	1 M KOH	1.50	0.27	280 @ 10 mA/cm^2	17
Exfoliated Ni-Fe nanosheets on GCE	1 M KOH	1.49	0.26	300 @ 10 mA/cm^2	6
Exfoliated Ni-Co nanosheets on GCE	1 M KOH	1.52	0.29	385@ 10 mA/cm^2	6
Exfoliated Co-Co nanosheets on GCE	1 M KOH	1.53	0.30	390 @ 10 mA/cm^2	6
Fe-Ni nanoparticles on GCE	1 M NaOH	1.40	0.17	256 @ 1 mA/cm^2 311 @ 10 mA/cm^2	18
Fe-$Ni_{4.34}$ on FeNi foil	1 M KOH	1.49	0.26	283 @ 10 mA/cm^2	26
NiCu-MOF nanosheet on Ni foam	1 M KOH	1.35	0.12	309 @ 10 mA/cm^2	27
3D Cu-Ni oxide on Ni foam	1 M NaOH	1.42	0.19	319 @ 10 mA/cm^2	28
Ir-Ni oxide thin film	0.1 M $HClO_4$	1.49	0.26	-	29
Ni-Ir thin film	0.1 M KOH	1.48	0.25	-	30
NiO-Fe on Ni foam	1 M KOH	1.46	0.23	240 @ 10 mA/cm^2	31
2D Ir-Ni oxide nanoframes	0.1 M $HClO_4$	1.50	0.27	-	32
$NiCo_{2.7}(OH)_x$ Amorphous double hydroxide	1 M KOH	1.48	0.25	350 @ 10 mA/cm^2	33
3D FeCoW	1 M KOH	1.42	0.19	191 @ 10 mA/cm^2	34
CNTs or carbon fiber supported					
NiFe-LDH/CNT	1 M KOH	1.45	0.22	149 @ 10 mA/cm^2	19
M-CNTs-Arc	1 M KOH	1.48	0.25	152 @ 10 mA/cm^2	20
$NiFeO_x$/CFP	1 M KOH	1.43	0.20	146 @ 10 mA/cm^2	21
20%Ir/C	1 M KOH	1.50	0.27	152 @ 10 mA/cm^2	22
FeNi on N-doped CNT	0.1 M KOH	1.59	0.36	810 @ 10 mA/cm^2	35
$Co_6Mo_6C_2$ on N-doped reduced graphene oxide film	1 M KOH	1.46	0.23	260 @ 10 mA/cm^2	36
Other					

Fe nanoparticles	1 M NaOH	1.56	0.33	421 @ 1 mA/cm^2	18
Ni nanoparticles	1 M NaOH	1.34	0.11	476 @ 1 mA/cm^2	18
Ni-FeO_x/C (69:31) nanoparticle on carbon black	1 M KOH	1.41	0.18	280 @ 10 mA/cm^2	23
Ir/C catalyst	0.1 M KOH	1.50	0.27	390 @ 30 mA/cm^2	12
NiFe phosphide nanoparticles	1 M KOH	1.51	0.28	270 @ 10 mA/cm^2	37
$NiCuO_x$ nanoparticles	1 M Na2CO3	1.55	0.32	680 @ 5 mA/cm^2	38
Ni-Cu nanoparticles in MOF	1 M KOH	1.68	0.45	640 @ 6 mA/cm^2	39
Ni@Pt core-shell nanoplates	1 M KOH	1.51	0.28	330 @ 10 mA/cm^2	40
CoNiPO	1 M KOH	1.49	0.26	320 @ 10 mA/cm^2	41
Ni-Co oxide hollow nanosponges	0.1 M KOH	1.50	0.27	362 @ 10 mA/cm^2	42
$Ni_{0.6}Co_{1.4}P$ nanocages	1 M KOH	1.52	0.29	300 @ 10 mA/cm^2	43
Nanoporous $(Co_{1-x}Fe_x)_2P$	1 M KOH	1.49	0.26	64 @ 10 mA/cm^2	44
Nanoporous Co_3Ni_1P	1 M KOH	1.48	0.25	281 @ 10 mA/cm^2	45

Table S2: Summary of performance of various OER electrocatalysts reported in the literature arranged by catalyst family.

References:

(1) L. Argueta-Figueroa, T. A. Morales-Luckie, R. J. Scougall-Vilchis, O. F. Olea-Mejia, *Prog. Nat. Sci. Mater.* 2014, ***24*,** 321-328.

(2) X. Gao, Y. Lu, M. Liu, S. He, W. Chen, *J. Mat. Chem. C* **2015,** *3*, 4050-4056.

(3) Y. C. Huang, Z. Getahun, Y. Zhu, J. Klemke, W. DeGrado, W. F. Gai, F., *Proc. Natl. Acad. Sci.* **2002**, *99*, 2788-2793.

(4) R. Forgie, G. Bugosh, C. K. Neyerlin, Z. Liu, P. Strasser, *Electrochem. Solid State Lett.* **2010**, *13*, B36-B39.

(5) C. Dong, X. Yuan, X. Wang, X. Liu, W. Dong, R. Wang, Y. Duan, F. Huang, *J. Mater. Chem. A* **2016**, *4*, 11292–11298.

(6) F. Song, X. Hu, Catalysis. *Nat. Commun.* **2014**, *5*, 1–9.

(7) K. Liu, C. Zhang, Y. Sun, G. Zhang, X. Shen, F. Zou, H. Zhang, Z. Wu, C. E. Wegener, C. J. Taubert, *ACS Nano* **2018**, *12*, 158–167.

(8) S. Hirai, S. Yagi, A. Seno, M. Fujioka, T. Ohno, T. Matsuda, *RSC Adv.* **2016**, *6*, 2019–2023.

(9) A. J. Koza, Z. He, S.A. Miller, A. J. Switzer, *Chem. Mater.* **2012**, *24*, 3567–3573.

(10) W.T. Kim, A. M. Woo, M. Regis, S. K. Choi, *J. Phys. Chem. Lett.* **2014**, *5*, 2370–2374.

(11) R. Subbaraman, D. Tripkovic, C. K., Chang, D. Strmcnik, P. A., Paulikas, P. Hirunsit, M. Chan, J. Greeley, V. Stamenkovic, M. N. Markovic, Nat. *Mater.* **2012**, *11*, 550–557.

(12) Z. Lu, W. Xu; W. Zhu, Q. Yang, X. Lei, J. Liu, Y. Li, X. Sun, X. Duan, *Chem. Commun.* **2014**, *50*, 6479–6482.

(13) Y. Zhang, B. Cui, C. Zhao, H. Lin, J. Li, *Phys. Chem. Chem. Phys.* **2013**, *15*, 7363–7369.

(14) X. Zou, A. Goswami, T. Asefa, *J. Am. Chem. Soc.* **2013**, *135*, 17242–17245.

(15) F. Yang, K. Sliozberg, I. Sinev, H. Antoni, A. Bïhr, K. Ollegott, W. Xia, J. Masa, W. Grïnert, R. B. Cuenya, *Chem. Sus. Chem.* **2017**, *10*, 156–165.

(16) Z. Lu, L. Qian, Y. Tian, Y. Li, X. Sun, X. Duan, *Chem. Commun.* **2016**, *52*, 908–911.

(17) S. Li, Y. Wang, S. Peng, L. Zhang, M. A. Al- Enizi, H. Zhang, X. Sun, G. Zheng, *Energy Mater*. **2016**, *6*, 1501661-1501667.

(18) L. S. Candelaria, M. N. Bedford, J. T. Woehl, S. N. Rentz, R. A. Showalter, S. Pylypenko, A. B. Bunker, S. Lee, B. Reinhart, Y. Ren*ACS Catal.* **2017**, *7*, 365–379.

(19) M. Gong, Y. Li, H. Wang, Y. Liang, Z. J. Wu, J. Zhou, J. Wang, T. Regier, F. Wei, H. Dai, *J. Am. Chem. Soc.* **2013**, *135*, 8452–8455.

(20) Y. Cheng, C. Liu, H. Cheng, P. S. Jiang, *ACS Appl. Mater. Interfaces* **2014**, *6*, 10089–10098.

(21) H. Wang, H. Lee, Y. Deng, Z. Lu, P. Hsu, Y. Liu, D. Lin, Y. Cui, *Nat. Commun.* **2015**, *6*, 7261.

(22) Y. Liu, H. Wang, D. Lin, C. Liu, P. Hsu, W. Liu, W. Chen, Y. Cui, *Energy Environ. Sci.* **2015**, *8*, 1719–1724.

(23) Y. Qiu, L. Xin, W. Li, *Langmuir* **2014**, *30*, 7893–7901.

(24) S. Hyun, S. Shanmugam, *ACS Omega* **2018**, 3, 8621-8630.

(25) K. W. Gao, Q. J. Chi, B. Z. Wang, H. J. Lin, P. D. Liu, B. J. Zeng, F. J. Yu, L. Wang, M. Y. Chai, B. Dong, *J. Colloid Interface Sci*. **2019**, 537, 11-19.

(26) Y. U. Qazi, Z. C. Yuan, N. Ullah, F.Y. Jiang, M. Imran, A. Zeb, J. S. Zhao, R. Javaid, W. A. Xu, *ACS. Appl. Mater. Interfaces*. **2017**, 9, 28627-28634.

(27) X. Zheng, X. Song, X. Wang, Z. Zhang, Z. Sun, Y. Guo, *New J. Chem*. 2018, 42, 8346-8350.

(28) C. Li, B. Zhang, Y. Li, S. Hao, X. Cao, G. Yang, J. Wu, Y. Huang, *Appl. Catal. B*. **2019**, 244, 56-62.

(29) T. Reier, Z. Pawolek, S. Cherevko, M. Bruns, T. Jones, D. Teschner, S. Selve, A. Bergmann, N. H. Nong, R. Schlogl, J.K. Mayrhofer, P. Strasser, *JACS* **2015**, 137, 13031-13040.

(30) E. Ozer, I. Sinev, M. A. Mingers, J. Araujo, T. Kropp, M. Mavrikakis, J. J. K. Mayrhofer, R. B. Cuenya, P. Strasser, *Surfaces*, **2018**, 1, 165-186.

(31) F. Song, M. M. Busch, B. Lassalle-Kaiser, S. C. Hsu, E. Petkucheva, M. Bensimon, M. H. Chen, C. Corminboeuf, X. Hu, *ACS Cent. Sci*. **2019**, 5, 558-568.

(32) F. Godinez-Salomon, L. Albiter, M. S. Alia, S.B. Pivovar, E. L. Camacho-Forero, B.P. Balbuena, R. Mendoza-Cruz, M. J. Arellano-Jimenez, C. P. Rhodes, *ACS Catal*. **2018**, 8, 10498-10520.

(33) J. Nai, H. Yin, T. You, L. Zheng, J. Zhang, P. Wang, Z. Jin, Y. Tian, J. Liu, Z. Tang, L. Guo, *Adv. Energy Mater*. **2015**, 5, 1401880.

(34) B. Zhang, X. Zheng, O. Voznyy, R. Comin, M. Bajdich, M. Garcia-Melchor, L. Han, J. Xu, M. Liu, L. Zheng, F. P. Garcia de Arquer, C. T. Dinh, F. Fan, M. Yuan, E. Yassitepe, N. Chen, T. Regier, P. Liu, Y. Li, P. De Luna, A. Janmohamed, H. L. Xin, H. Yang, A. Vojvodic, E. H. Sargent, *Science,* **2016**, 352, 333-337.

(35) Y. Cheng, S. He, P. J. Veder, R. De Marco, Z. S. Yang, S. P. Jiang, *ChemElectroChem* **2019**, 6, 3478-3487.

(36) Y.J. Tang, C.H Liuk, W. Huang, X. L. Wang, L. Z. Dong, S. L. Li, Y. Q. Lan, *Appl. Mater. Interface*. **2017**, 9, 16977-16985.

(37) W. K. Gao, J. Q. Chi, Z. B. Wang, J. H. Lin, D. P. Liu, J. B. Zeng, J. F. Yu, L. Wang, Y. M. Chai, B. Dong, *J. Colloid Interface Sci*. **2019**, 537, 11-19.

(38) L. Wang, X. Ge, Y. Li, J. Liu, L. Huang, L. Feng, Y. Wang, *J. Mater. Chem. A*. **2017**, 5, 4331-4334.

(39) X. Ma, K. Qi, S. Wei, L. Zhang, X. Cui, *J. Alloys Compd*. **2019**, 770, 236-242.

(40) F. Wang, G. Chen, X. Liu, F. Chen, H. Wan, L. Ni, N. Zhang, R. Ma, G. Qiu, *ACS Sustainable Chem. Eng*. **2018**, 7, 341-349.

(41) J. Wu, L. Lin, F. J Morvan, J. Du, W. Fan, *Inorg. Chem. Front*. **2019**, 6, 2014-2023.

(42) C. Zhu, D. Wen, S. Leubner, M. Oschatz, W. Liu, M. Holzschuh, F. Simon, S. Kaskel, A. Eychmuller, *Chem. Commun*. **2015**, 51, 7851-7854.

(43) B. Qiu, L. Cai, Y. Wang, Z. Lin, Y. Zuo, M. Wang, Y. Chai, *Adv. Funct. Mater*. **2018**, 28, 1706008.

(44) Y. Tan, H. Wang, P. Liu, Y. Shen, C. Cheng, A. Hirata, T. Fujita, Z. Tang, M. Chen, *Energy Environ. Sci*. **2016**, 9, 2257-2261.

(45) S. Fu, C. Zhu, J. Song, M. H. Engelhard, X. Li, D. Du, Y. Lin, *ACS Energy Lett*. **2016**, 1, 792-796.